

**NASA CONTRACTOR
REPORT**

NASA CR-2053



NASA CR-2053

0061161

TECH LIBRARY KAFB, NM

LOAN COPY: RETURN TO
AFWL (DOUL)
KIRTLAND AFB, N. M.

INDUCTION TORCHES AND LOW FREQUENCY TESTS

by John W. Poole and Charles E. Vogel

Prepared by

TAFD DIVISION

HUMPHREYS CORPORATION

Concord, N.H. 03301

for Lewis Research Center

NATIONAL AERONAUTICS AND SPACE ADMINISTRATION • WASHINGTON, D. C. • MAY 1972



0061161

1. Report No. CR-2053		2. Government Accession No.		3. Recipient's Catalog No.	
4. Title and Subtitle INDUCTION TORCHES AND LOW FREQUENCY TESTS				5. Report Date May 1972	
				6. Performing Organization Code	
7. Author(s) John W. Poole and Charles E. Vogel				8. Performing Organization Report No. None	
				10. Work Unit No.	
9. Performing Organization Name and Address TAFI Division Humphreys Corporation Concord, New Hampshire 03301				11. Contract or Grant No. NAS 3-14423	
				13. Type of Report and Period Covered Contractor Report	
12. Sponsoring Agency Name and Address National Aeronautics and Space Administration Washington, D. C. 20546				14. Sponsoring Agency Code	
15. Supplementary Notes Project Manager, Chester D. Lanzo, Nuclear Systems Division, NASA Lewis Research Center, Cleveland, Ohio					
16. Abstract Three induction coupled plasma torches were operated at 9600 Hz to determine specific operating parameters and supply data for future GCNR simulation studies. Two air cooled torches, one 16 cm i. d. and one 30 cm i. d., and one water cooled torch, 14 cm i. d., were tested. Complete energy balances for the operating systems were obtained during operation. A series of operating points including pressures from 30 torr to 1 atmosphere, power levels up to 343 kW, and gas flows from 1.1 to 35 g/sec were documented. Complete operating data for approximately thirty runs are presented along with graphs of significant operating parameters.					
17. Key Words (Suggested by Author(s)) Induction heated gases Gas core reactors Plasmas Radiofrequency heating High-temperature gases				18. Distribution Statement Unclassified-unlimited	
19. Security Classif. (of this report) Unclassified		20. Security Classif. (of this page) Unclassified		21. No. of Pages 41	
				22. Price* \$3.00	

TABLE OF CONTENTS

	Page
I. SUMMARY.....	1
II. INTRODUCTION.....	1
III. DESCRIPTION OF TORCHES.....	2
IV. DESCRIPTION OF TEST FACILITY.....	4
V. INSTRUMENTATION AND MEASUREMENT TECHNIQUES.....	5
VI. TESTING SEQUENCE.....	7
VII. TABLE OF RESULTS AND SAMPLE CALCULATIONS.....	8
VIII. DISCUSSION OF RESULTS.....	9
Significance of Gas Flows.....	9
Significance of Electrical Measurements.....	10
Nitrogen Injection.....	10
Significance of Torch Size.....	11
IX. CONCLUSIONS.....	12
APPENDIX A -	
SAMPLE DATA REDUCTION CALCULATIONS (Run 61A).....	14
REFERENCES.....	16
TABLES I - III.....	17
FIGURES.....	20

INDUCTION TORCHES AND LOW FREQUENCY TESTS

By John W. Poole and Charles E. Vogel

I. SUMMARY

An experimental program was conducted with the goal of obtaining complete operating information for three plasma generators operating at 9600 Hz, the objective being to establish important design and operating parameters for future Gas Core Nuclear Rocket simulator work at higher power levels.

Operating information is reported for a 14 cm i.d. water cooled torch and a 30 cm i.d. air cooled torch. Data covers a pressure range from 30 torr to 1 atmosphere. Argon was the primary operating gas with flow rates ranging from 1.1 g/sec to 35 g/sec. Nitrogen was introduced during several runs at a variety of operating conditions, and always caused arc extinction. The test power levels ranged up to 343 kW when working with the water cooled torch.

Reported results include plots of the minimum power required to sustain a plasma as a function of pressure level and gas flow. The effect of the gas flow rate, gas injection pattern, and the electrical coupling efficiency on minimum sustaining power is discussed. Several reasons for extinguishment with small nitrogen additions are also discussed.

The tests have provided a more comprehensive understanding of plasma torch operation at low frequency. The highly successful operation of the 30 cm i.d. torch demonstrated the advantage of high load to reference depth ratios. A technique for calculating the performance of various induction coupled plasma generator configurations at low frequency is being developed, and shows promise of being very useful in future high powered simulator programs.

II. INTRODUCTION

The objective of this program was to obtain detailed operating information for induction plasma generators powered at

9600 Hz. To accomplish this the previously tested 16 cm and 30 cm (i.d.) uncooled torches were modified and reconditioned, and a new 14 cm water cooled torch was constructed. These torches were operated on a 350 kW 9600 Hz power supply at various gas flow rates and over a pressure range of 30 torr to 1 atmosphere. Instrumentation was provided to obtain continuous heat balances throughout each run.

Of particular interest was the highly successful operation of the 30 cm torch which operated at significantly lower powers than the 16 cm unit. A second important result was the effect of nitrogen addition to argon plasmas during operation. These two items and the heat balance results are reported and analyzed in various sections of this report. Implications of the results to future low frequency work at higher power are also discussed. As a result of this work, an analytical technique is being developed which will permit prediction of high powered, low frequency plasma performance.

III. DESCRIPTION OF TORCHES

The three torches tested were selected to bracket the predicted optimal torch geometry for a plasma generator at 9600 Hz. The 16 cm and 30 cm uncooled torches were modified versions of units used on a previous contract in 1970.¹ A new 14 cm water cooled torch was designed to allow continuous operation at high power levels and to provide for complete heat balances by measuring radiation and conduction losses to the torch wall. The 14 cm cooled and 16 cm uncooled torches used the same five-turn work coil and, consequently, the buss and capacitor setup was identical. The larger six-turn coil used with the 30 cm torch had been operated previously at 960 Hz. The connections to this coil were modified to permit adaption to the buss of the 9600 Hz power unit.

The cross section of the 16 cm uncooled torch is shown in Figure 1. The bottom section of the torch base and the gas injector had been used previously.¹ The next section of the base was designed to be common to this uncooled torch and the water cooled version. The gas seal at the base of the torch was accomplished with o-rings. The wall of the plasma chamber was a 71.1 cm long sleeve of opaque fused quartz with an 0.8 cm wall. The top of the torch consisted of a water cooled

copper ring which supported a pyrex sight port and provided an exit for plasma gases. The five-turn work coil had been operated previously.¹ The lamination stacks had been used previously. Edge cooling was added to the two stacks adjacent to the power leads to prevent overheating.

The 14 cm water cooled torch shown in Figure 2 was selected as the primary test unit since continuous operation permitted simplified collection of data over a wide range of pressures and powers without shut down. Because of a slightly different diameter of the torch wall a diffuser section was added to expand the flow smoothly from the 8.25 cm o.d. gas injector to the torch wall (clear fused quartz 14 cm i.d. by 45.7 cm long). The outside shell of the torch was constructed of acrylic with excellent light transmission characteristics. One inherent weakness of the acrylic for this application is the relatively high absorption of ultra-violet which resulted in surface degradation after a number of runs. Since this item was relatively inexpensive, the problem was overcome by replacing the wall when excessive degradation occurred.

The exit section of the torch provided an end-on view port, connection for cooling, and an exhaust gas calorimeter. This section was supported on four large fiberglass reinforced epoxy rods which not only supported the weight of the top section but also held the torch together when water pressure was applied. These tie bolts were protected from the high radiation level present immediately outside of the torch with high reflectivity fiberglass tape.

A water cooled grid of copper tubing covered half of the aperture under the sight port to reduce the radiation impinging on the sight port and prevent impingement of hot gases during extended runs at reduced pressure. For atmospheric pressure tests the sight port was removed. The exhaust gas calorimeter permitted continuous operation and complete system heat balance measurements under vacuum conditions without overheating the vacuum pump. A full description of this calorimeter is given in Reference 1.

Figure 2 shows the laminations in place around the coil of the 14 cm torch. The radiation from the plasma produced such extreme heating of the epoxy encapsulant, even with shielding, that an attempt was made to operate at lower flux density without the laminations. This was successful at a penalty of about 12%

in operating power at the minimum sustaining point. As a result of this, the bulk of the runs were made without laminations, as noted in Table I.

A cross section of the 30 cm torch is shown in Figure 3. The base was a special gas injector that provided radial and tangential gas flow. A metallic section positioned between the exit end of the quartz wall and the sight port was modified for this testing series to provide for attachment of the exhaust gas calorimeter. As with the 14 cm torch, this device permitted longer run times at sub-atmospheric pressures.

Since the induction coil had been used previously on a different power supply, new connections were required for the coil to adapt it to the busses at the 9600 Hz test facility. Due to the large inductance of this six-turn 35.6 cm i.d. coil, the coil currents during tests with this device were much lower than those experienced with the five-turn 18.4 cm i.d. coil used with the 14 cm and 16 cm torches. Consequently, the interconnecting buss did not have to be water cooled. As detailed in Figure 3, steel laminations were positioned around the coil to increase the flux density. As with the smaller diameter torch, it was possible to operate this torch without laminations. Run No. 84, reported in Table I, shows typical operating conditions of this torch with the laminations removed.

IV. DESCRIPTION OF TEST FACILITY

The tests covered by this report were conducted at the TOCCO Division of Park Ohio Industries, Inc., Cleveland, Ohio. Figure 4 shows the test setup with (proceeding from right to left) the 4 MHz ignition power supply, the test instrumentation and controls, and the plasma generator test station. The primary power control was located approximately thirty feet from the test supervisor. The test crew included a power supply operator, a test supervisor who controlled the instrumentation and recording equipment, a technician who applied the starting power pulse and regulated the gas pressure during a run, and a cameraman who recorded the runs with still photographs plus regular and high speed movies.

The 9600 Hz power was supplied by two MG sets rated at 175 kW output each. These could be operated individually or in parallel for a total rated output of 350 kW. Power from the MG sets was

bussed overhead and brought down to the test bay on 500 MCM cables. A water cooled tapped autotransformer was used for impedance matching. Electrical metering included a voltmeter and ammeter connected to the input leads of the autotransformer. Power connections to the capacitor bank along with the vertical buss leading to the work coil (with the water cooling lines in evidence) are shown in Figure 5. The capacitors were connected in two series banks in order to operate within their 800 volt rating. These capacitor banks and various sections of the buss work were water cooled with fourteen separate cooling loops. The heat loss in these loops was measured during one long test run (Run No. 57) and losses during other runs were considered proportional.

The control station for the 9600 Hz power permitted either one or both of the MG sets to be connected to the buss with appropriate power control, and provided complete electrical metering. It was not possible, however, to add the second MG set to the line after the first one was under load. For dual MG set operation both power supplies had to be loaded together. A significant limitation of the dual MG operation was that the voltage prior to ignition had to be set in excess of 70%, or about 560 volts in order to properly synchronize the two sets. This voltage caused a power surge and resultant torch failure when low starting gas flows were used. This limitation and occasional difficulties in communication between the test controller and the power supply operator were the only problems encountered in utilizing the facility.

V. INSTRUMENTATION AND MEASUREMENT TECHNIQUES

A fourteen channel Honeywell visicorder was used to provide a continuous record of each run. This allowed reliable data acquisition even during the fifteen to thirty second runs characteristic of uncooled torch operation. Figure 6 is a typical trace obtained during the ignition sequence for one of the 14 cm torch runs, Figure 7 is the ignition sequence for the 30 cm torch, and Figure 8 shows the power reduction for a minimum sustaining power determination at the end of Run No. 61. Figure 9 is a photograph of the complete instrumentation setup.

The electrical power measurement signals were conditioned by a special millivolt converter. This provided a 0 to 10 millivolt output for full scale range on the voltmeter, kilowatt and

KVAR meters. By referring to the standard power triangle calculation it was possible to solve for the phase angle and the MG current corresponding to any given set of the other three measurements. This calculation was made for all of the data points presented in Table I.

The heat loss determination was accomplished by using rotameters in the three cooling water circuits and special thermistor temperature sensors in the ΔT bridge circuits which measured the temperature rise across each of the circuits. These three ΔT systems operated very well for most of the tests although the calorimeter channel became inoperative near the end of the testing series. The coil circuit instrumentation had a 2.5 sec response delay which was taken into consideration in utilizing the measurements from the visicorder traces. Periodic checking revealed that the water flow rate did not vary significantly during the testing period and was considered to be a constant.

The radiant energy from the torch was measured using a calibrated Hy-Cal Pyrheliometer Model 8401. In order to achieve a suitable signal for the visicorder, the pyrheliometer signal was connected to a Keithley microvoltmeter operating on the 10 millivolt scale. The Keithley provides a recorder output which is proportional to the meter deflection and this was run through a voltage divider network to provide the appropriate input for the visicorder. The Keithley has a risetime of one second which reduced the ability of the radiation sensor to record transient events.

One other significant test variable was the gas flow rate through the torch. This was monitored on a flowmeter panel arranged to measure the input of two different gases to each set of ports in the gas injector. As can be noted in Figure 9, one rheostat for each flowmeter was located above the gas metering and control panel. These were used to control a signal to the visicorder. The operating technique was to set the flow desired on a particular flowmeter and then set the rheostat at a percentage equivalent to the percent flow on the corresponding flowmeter. As the test was run, the gas flow toggle switch was tripped along with a switch that applied power to the appropriate rheostat. This fed the voltage to the recorder and indicated the timing and magnitude of a particular flow. Pressure measurements were observed on a Wallace and Tiernan gauge and a calibrated altimeter.

A Tektronix Model 545A dual trace oscilloscope was used as a diagnostic tool for several measurements. It was particularly useful in determining the phasing problem with the MG sets discussed elsewhere in this report.

VI. TESTING SEQUENCE

Table I presents detailed data for the significant tests conducted in a series of tests which commenced on August 3, 1971. A total of 84 individual runs were made. The first 51 runs were used to debug the equipment, calibrate the various instrumentation, and determine the operating limits of the torches. Figure 10 is a photograph of the 16 cm air cooled torch which was used primarily for system checkout. Figure 11 is a photograph of the 14 cm water cooled torch set up and ready to run. This device was the primary test article during the testing sequence. Figure 12 is another photograph of the 14 cm torch but shows it during operation. Table I details which torch was used for each run, whether laminations were installed, and other modifications which may have been employed.

The ignition technique used for most tests involved pumping the torch down to approximately 0.1 torr, back filling with argon, pumping down again, and then establishing an argon flow to maintain torch pressure at approximately 1 torr. A glow discharge was then established within the torch by connecting a 4 MHz oscillator across the torch base and an electrode positioned on top of the exit sight port. The actual placement of the electrodes for this ignition glow is not critical as long as both electrodes are not in direct contact with the gas in the torch cavity.

An alternate ignition technique was also developed wherein a glow discharge could be established at 0.05 torr with the 9600 Hz power applied to the coil.

VII. TABLE OF RESULTS AND SAMPLE CALCULATIONS

Table I is a compilation of the variables and operating characteristics for the significant test runs. Runs 1 to 51 are not presented since they were used to calibrate instrumentation, select gas flow rates, perfect starting technique, and establish proper control of the 9600 Hz power.

Appendix A demonstrates typical data reduction calculations. The sample calculations presented are for Run No. 61A. Coil voltage was determined by actual measurement during a number of runs to establish the ratio between coil and input voltage for particular autotransformer connections.

The variation of MSP* and power delivered to the plasma gas for the 14 cm and 30 cm torches under various test conditions are shown in Figures 15 through 18. The MSP was determined by reducing the power to extinguishment at a fixed gas flow from a stable operating point.

Figure 15 shows a smooth trend of increasing power requirement with increasing pressure for the 14 cm torch. One factor affecting this trend is the shorter mean free path of charged particles at increasing pressure, thereby requiring higher magnetic field strength to maintain ionizing energy. A second factor is the increased gas flow which is required since it is working against a fixed displacement of the vacuum pump. The effect of the gas flow on the plasma load diameter is discussed at length on page 9. Radiation losses may also be involved since they would be expected to be higher with increased pressure. Counteracting this, however, is the fact that the plasma is larger in diameter at low pressure and therefore the radiating plasma area is greater. Quantitative data for these tests has not been generated.

It can be noted that the MSP for the small torch is roughly double that of the large torch. One major factor causing this result was the reduced I^2R heating in the cross section of the larger coil. A second factor was that the load to reference depth ratio was greatly improved in the larger torch. A more detailed discussion of the effect of this relationship is included on page 10 of this report.

Figure 16 presents data from the same runs as Figure 15 but shows energy delivered to the plasma as a function of pressure. Within the accuracy of the measurements made, the power to the gas was identical for the two torches. Since the gas flows were the same at a given pressure level, one would expect the only differences to be caused by different load to reference depth and load to coil ratios, and possibly different radiant and conduction losses. It appears to be a coincidence that the

*MSP, "Minimum Sustaining Power" is defined as the lowest MG power output at which a plasma can be sustained at a given set of conditions.

increased efficiency of the larger torch caused the two configurations to behave very much the same electrically.

Figure 17 shows the MSP as a function of gas flow for atmospheric pressure operation on argon. The approximate two to one relationship between the 14 cm and the 30 cm torches is again apparent, as it was for various pressures shown in Figure 15. Once again this apparent anomaly in results with the larger torch operating at lower powers than the smaller torch is a result of the increased efficiency of the larger torch. Figure 18 presents data from the same runs as Figure 17 but shows energy delivered to the plasma as a function of torch gas flow.

VIII. DISCUSSION OF RESULTS

Significance of Gas Flows

It is common knowledge that the arc zone in a plasma device can be displaced or distorted by improper introduction of gases. For stable operation it is imperative that a properly designed and operated gas injector be used. All of the torches discussed in this report have provision for radial and swirl (tangential) injection of gases. Even with these two sets of injection ports it is possible to vary the stability and electrical response of a plasma by altering the ratios of gas injection through the two sets of ports. For the 14 cm and 16 cm torches an effort was made during Run No. 37 to determine the optimum flow relationship between the radial and tangential gas injection ports. During this run the only visible access to the arc was through the sight port in the exit end of the torch and the observed diameter and apparent stability of the arc were used as a criteria for judging performance. It was determined that a gas flow ratio of 120 radial to 100 tangential produced the largest and most stable plasma.

While Figures 17 and 18 demonstrate the power requirement increase with increased gas flow, these curves cannot be extrapolated and used directly for the design of the GCNR. These particular devices did not contain a permeable wall or central fuel injection separate from the remainder of the gas flow. These results, however, are extremely valuable in designing large high powered induction devices which can be used to simulate the GCNR.

Significance of Electrical Measurements

It has long been considered desirable to use the electrical measurements made on a particular plasma generator to predict temperature and size of the plasma load. Reference 1 describes a technique for determining the optimum number of turns for a coil to match the particular plasma load and Reference 2 presents the equations which can be used to relate the measured variables of torch operation with the characteristics of the load. A series of solutions to these equations for the 30 cm torch are presented in Table II. For these calculations the diameter of the coil, the number of turns, and the voltage across the coil were kept constant, however, the load diameter and resistivity were allowed to change. The table shows that as the plasma resistivity decreases (equivalent to a temperature increase) the coil efficiency and the power coupled into the load increase. It can also be seen in Table II that as the diameter of the load is increased, the power coupled into the load increases significantly. Table III presents similar calculations for the 14 cm torch and shows the marked reduction in efficiency.

It now appears possible to use these types of calculations to match the results obtained from a particular torch run and determine the size and conductivity (temperature) of the load. Since only one load diameter and resistivity combination will completely match a particular set of measured electrical variables and coil heat loss, the capability to perform this type of calculation will be extremely important when operating plasmas inside of the opaque GCNR simulator.

Nitrogen Injection

Since testing of the GCNR simulator will require operation with various gas mixtures, a number of tests were conducted in which nitrogen was added to the argon gas stream. Five of these runs are included in Table I. It can be noted that a maximum of 1.6% nitrogen was added during Run No. 68. This is just below what would be expected at the power levels available. TAFA's experience indicates that the MSP for 100% nitrogen at 9600 Hz is approximately 4000 kW compared to about 100 kW or less for argon, therefore, only a small addition of nitrogen can

be tolerated in an argon plasma without significantly increased power. Several possible explanations for the high power requirements with nitrogen injection are discussed in the following paragraphs.

The presence of nitrogen produces two second order effects that both reduce the electrical coupling efficiency into the load. The first one involves the dissociation of nitrogen which produces a peak in its thermal conductivity at about 8000°K. This results in an increase in heat loss from the side of the plasma causing a shrinking of the ionized zone. This results in a reduction in coupling efficiency by reducing the effective diameter and length of the load. The second effect is that nitrogen has a somewhat higher resistivity than argon which tends to increase the reference depth of the plasma. This also reduces the coupling efficiency by reducing the load to reference depth ratio.

On page 332 of Reference 3, it is indicated that the visual radiation from a nitrogen arc is about four times the value for argon. While this does not affect the electrical efficiency directly, it is another increased loss mechanism.

Figure 19 shows the elastic collision cross section for electrons in argon and nitrogen as a function of electron energy. It can be noted that argon is almost transparent to electrons at an energy level below 1 eV. As the energy level goes up to approximately 2 eV, the difference between the cross section for nitrogen and argon remains about five to one or greater. The significance of this factor is that with nitrogen present in the torch the electrons will have a much shorter mean free path and will not travel as far in the direction of the field during a given cycle. This will make it more difficult to impart enough energy to the electrons to obtain ionized collisions. A more complete description of this phenomena can be found in Reference 4.

Significance of Torch Size

The parts played by the load to coil diameter and load to reference depth ratios when inductively coupling energy into a conductive material have long been recognized. Figure 20 shows the variation of a coupling coefficient, or load resistance factor,

as a function of the load to reference depth ratio. The curve shows that at a load to reference depth ratio below about 3.5 the coefficient drops off rapidly.

The calculation for the 14 cm torch indicates that it had a plasma diameter for reference depth ratio of about one whereas the 30 cm torch had a ratio of nearly three. This fact, at least in part, helps to explain why the larger diameter torch ran at significantly higher efficiencies and therefore lower powers than the smaller diameter torch. It should be noted that the efficiency of a torch larger than 30 cm would not be expected to increase significantly, more power would also be required to operate such a device because of the increased radiative, conductive, and convective heat losses.

In addition to the increased coupling efficiency obtained in the 30 cm torch, significantly lower coil losses were also experienced in this device. The coil loss for the 14 cm torch was measured between 38 and 50% of the power applied to the buss depending on the specific load condition. One set of calculations using the equations previously discussed predicted a coil loss for this torch of 45%. Thus, both operating experience and the calculations indicated that this torch and coil is too small to operate efficiently at 9600 Hz. For the 30 cm diameter torch the coil losses ran at approximately 14% of the power applied to the buss. Calculations for this device substantiated the loss experienced during the tests and confirmed the observed results that the 30 cm torch should run at a total power input lower than the 14 cm torch. Once again it is important to point out that this condition would not persist if larger diameter torches were constructed. It is now possible, however, with the data now available to predict more accurately the optimum size for operating at minimum powers at 9600 Hz.

IX. CONCLUSIONS

The primary goal of this program to obtain complete operating information for particular plasma torch configurations at 9600 Hz was achieved. This data can now be used in the design and operation of subsequent GCNR simulators. Specific conclusions based on tests conducted are as follows.

1. Sufficient data is now available to permit the design of induction plasma devices for operation

at significantly higher powers than heretofore experienced.

2. The operating characteristic of low frequency plasmas, specifically at 9600 Hz, are now sufficiently understood to satisfactorily design large devices such as are required for GCNR simulation studies.
3. The primary role of electrical coupling characteristics as they relate to torch diameter, coil to reference depth ratio and coil configuration are now more fully understood and permit specific design of future devices.
4. Significant progress has been made toward designing and operating a device which closely simulates the GCNR.

APPENDIX A

SAMPLE DATA REDUCTION CALCULATIONS (RUN 61A)

Recorded Values: Reading at 31 sec into run

Capacitors Installed = 11,115 KVAR

MG volts 808

MG kW 195.8 kW = 185.0 Btu/sec

MG KVAR 27.3

Torch $\dot{w} = 78.2\%$ $\Delta T = 9.0^\circ\text{F}$

Calorimeter $\dot{w} = 42.4\%$ $\Delta T = 4.9^\circ\text{F}$

Coil $\dot{w} = 56.2\%$ $\Delta T = 35.8^\circ\text{F}$

Pyrheliometer 0.88 mV

Gas Flow 42.5% @ 102 psig argon

$$\dot{Q} = 876 \times .425 \sqrt{\frac{102 + 14.7}{14.7} \times \frac{.967}{1.38}} = 880 \text{ SCFH (11.6 g/sec)}$$

$$\text{Power angle } \phi = \tan^{-1} \frac{\text{KVAR}}{\text{kW}} = 8.4^\circ$$

$$I_{\text{MG}} = \frac{\text{kW}}{E_{\text{MG}} \cos \phi} = 232 \text{ amps}$$

$$\begin{aligned} \text{Coil voltage} &= E_{\text{MG}} \times \text{autotransformer turns ratio} \times \text{autotransformer efficiency} \\ &= 808 \times 1.50 \times .88 = 1067 \end{aligned}$$

$$\text{Volts/cm of arc} = \frac{\text{coil volts/coil turn}}{\text{arc length}} = \frac{1067/5}{\pi \times 11.4} = 5.9 \text{ volts/cm}$$

(11.4 cm diameter arc assumed for 14 cm i.d. torch, and 20.3 cm diameter assumed for 30 cm i.d. torch.)

$$\begin{aligned}
 \text{Coil current} &= \frac{\text{rated current}}{\text{capacitor @ 800 V}} \times \frac{\text{volts/capacitor bank}}{\text{rated volts/cap}} \\
 &\times \frac{\text{total KVAR/2 cap banks}}{450 \text{ KVAR/cap}} = 563 \times \frac{1067/2}{800} \times \frac{11,115/2}{450} \\
 &= 4628 \text{ amps}
 \end{aligned}$$

Heat Balance Losses:

$$\text{Loss} = \text{Rotameter reading (percent)} \times \text{full scale flow} \times \text{conversion factor from gpm to lb/sec} \times \Delta T \cdot ^\circ\text{F} = \text{Btu/sec}$$

Percent loss column is percent of MG power supplied.

\dot{Q}_{torch}	=	.782 x 28.3 x .139 x 9.0	=	27.7 Btu/sec	=	15.0%
\dot{Q}_{cal}	=	.424 x 28.3 x .139 x 4.9	=	8.38 " "	=	4.5
\dot{Q}_{coil}	=	.562 x 28.3 x .139 x 35.8	=	79.1 " "	=	42.8
\dot{Q}_{pyrh}	=	0.88 x 2 x 8.55 x 1.33	=	20.1 " "	=	10.8
\dot{Q}_{caps}	=	11,150 $\frac{(\frac{808 \times 1.32}{2})^2}{(800)^2} \times 1.6 \times .945$	=	7.47 " "	=	4.1
\dot{Q}_{buss}	=	Assumed proportional to input kW	=	5.25 " "	=	<u>2.8</u>
				Total Losses		80.0%

REFERENCES

1. Vogel, Charles E.; Poole, John W.; and Dundas, Peter H.: Radiation Measurements and Low Frequency and High Pressure Investigations of Induction Heated Plasma. NASA CR-1804, 1971.
2. Vaughan, J.T.; and Williamson, J.W.: Design of Induction Heating Coils for Cylindrical Nonmagnetic Loads, AIEE Paper No. 45-107.
3. Cobine, J.D.: Gaseous Conductors, Theory and Engineering Applications. Dover Publications, Inc., New York, 1958.
4. Nasser, E.: Fundamentals of Gaseous Ionization and Plasma Electronics. John Wiley - Interscience, New York, 1971.

TABLE II

CALCULATED ELECTRICAL PERFORMANCE OF 30 cm I.D. TORCH
(Coil Voltage - 1400 volts)

	Plasma Diameter					
	25.4 cm	22.9 cm	20.3 cm	17.8 cm	15.2 cm	12.7 cm
	$\rho_2 = 0.0813 \Omega\text{-cm (8400^\circ\text{K})}$					
1	165	109	71.8	47.4	32.2	23
2	92	87.7	81.1	71.	56.4	38.2
3	152	96	58.2	33.6	18.1	8.9
4	2025	2027	2035	2048	2067	2091
	$\rho_2 = 0.0711 \Omega\text{-cm (8700^\circ\text{K})}$					
1	195	127	82	53.4	35.4	24.9
2	93.	88.9	82.9	73.4	59.4	41.2
3	180	113	68	39.2	21.0	10.2
4	2074	2069	2070	2078	2092	2112
	$\rho_2 = 0.061 \Omega\text{-cm (8900^\circ\text{K})}$					
1	234	151	96.4	61.3	39.7	27.0
2	93.7	90.3	84.8	76.1	62.8	44.6
3	219	136	81.8	46.7	24.9	12.1
4	2128	2115	2110	2111	2120	2135
	$\rho_2 = 0.0508 \Omega\text{-cm (9300^\circ\text{K})}$					
1	291	185	116	72.4	45.5	30.0
2	94.6	91.7	86.9	79.1	66.6	48.8
3	275	169	100	57.2	30.3	14.6
4	2190	2169	2155	2149	2151	2160
	$\rho_2 = 0.0407 \Omega\text{-cm (9700^\circ\text{K})}$					
1	377	236	146	88.9	54.2	34.2
2	95.5	93.1	89.1	82.	71.1	54.
3	360	220	130	73.2	38.5	18.5
4	2261	2230	2206	2192	2186	2189
	$\rho_2 = 0.035 \Omega\text{-cm (10,400^\circ\text{K})}$					
1	415	296	196	116	68.5	41.0
2	95.6	94.1	91.4	85.8	76.2	60.5
3	397	279	179	100	52.2	24.8
4	2352	2303	2267	2243	2228	2222
	$\rho_2 = 0.0203 \Omega\text{-cm (11,900^\circ\text{K})}$					
1	493	346	242	171	96.6	54.3
2	95.9	94.6	92.6	89.8	82.3	69.
3	473	328	224	153	79.5	37.5
4	2468	2398	2345	2305	2279	2263

1 = Power to coil (kW)

2 = Coil efficiency (percent)

3 = Power to the plasma (kW)

4 = Coil current (amperes)

TABLE III

CALCULATED ELECTRICAL PERFORMANCE OF 14 cm I.D. TORCH
(Coil Voltage = 1200 Volts)

	12.7 cm	11.4 cm	Plasma Diameter			
			10.2 cm	8.9 cm	7.6 cm	6.35 cm
$\rho_2 = 0.0813 \Omega\text{-cm} (8400^\circ\text{K})$						
1	78.4	65.6	56.8	51.5	49.1	49.1
2	63.3	52.0	39.4	27.	16.3	8.5
3	49.6	34.1	22.4	13.9	8.02	4.2
4	3632	3801	3974	4153	4340	4538
$\rho_2 = 0.0711 \Omega\text{-cm} (8700^\circ\text{K})$						
1	91.5	74.9	63.4	56.1	52.4	51.4
2	66.1	55.0	42.4	29.5	18.1	9.5
3	60.5	41.2	26.9	16.5	9.48	4.9
4	3771	3930	4092	4260	4435	4620
$\rho_2 = 0.061 \Omega\text{-cm} (8900^\circ\text{K})$						
1	109.6	87.4	72.0	62.0	56.4	54.3
2	69.2	58.5	45.9	32.5	20.3	10.8
3	75.9	51.2	33.0	20.2	11.4	5.9
4	3932	4078	4226	4380	4541	4712
$\rho_2 = 0.0508 \Omega\text{-cm} (9300^\circ\text{K})$						
1	136	105	83.9	69.9	61.7	57.9
2	72.7	62.6	50.1	36.3	23.2	12.6
3	98.8	65.9	42.0	25.4	14.3	7.3
4	4124	4251	4382	4519	4663	4817
$\rho_2 = 0.0407 \Omega\text{-cm} (9700^\circ\text{K})$						
1	177	132	102	81.4	69.0	62.6
2	76.6	67.2	55.2	41.2	27.0	15.0
3	136	89.2	56.2	33.6	18.7	9.4
4	4359	4461	4569	4683	4806	4938
$\rho_2 = 0.0305 \Omega\text{-cm} (10,300^\circ\text{K})$						
1	250	179	131	99.7	80.2	69.3
2	81.0	72.8	61.7	47.8	32.6	18.7
3	202	131	80.9	47.6	26.1	13.0
4	4660	4727	4801	4885	4978	5084
$\rho_2 = 0.0203 \Omega\text{-cm} (11,900^\circ\text{K})$						
1	405	276	190	135	100	80.8
2	86.1	79.6	70.1	57.1	41.3	25.1
3	349	220	133	77.0	41.3	20.3
4	5072	5084	5108	5147	5200	5268

1 = Power to coil (kW)

3 = Power to the plasma (kW)

2 = Coil efficiency (percent)

4 = Coil current (amperes)

16 cm I.D. UNCOOLED TORCH

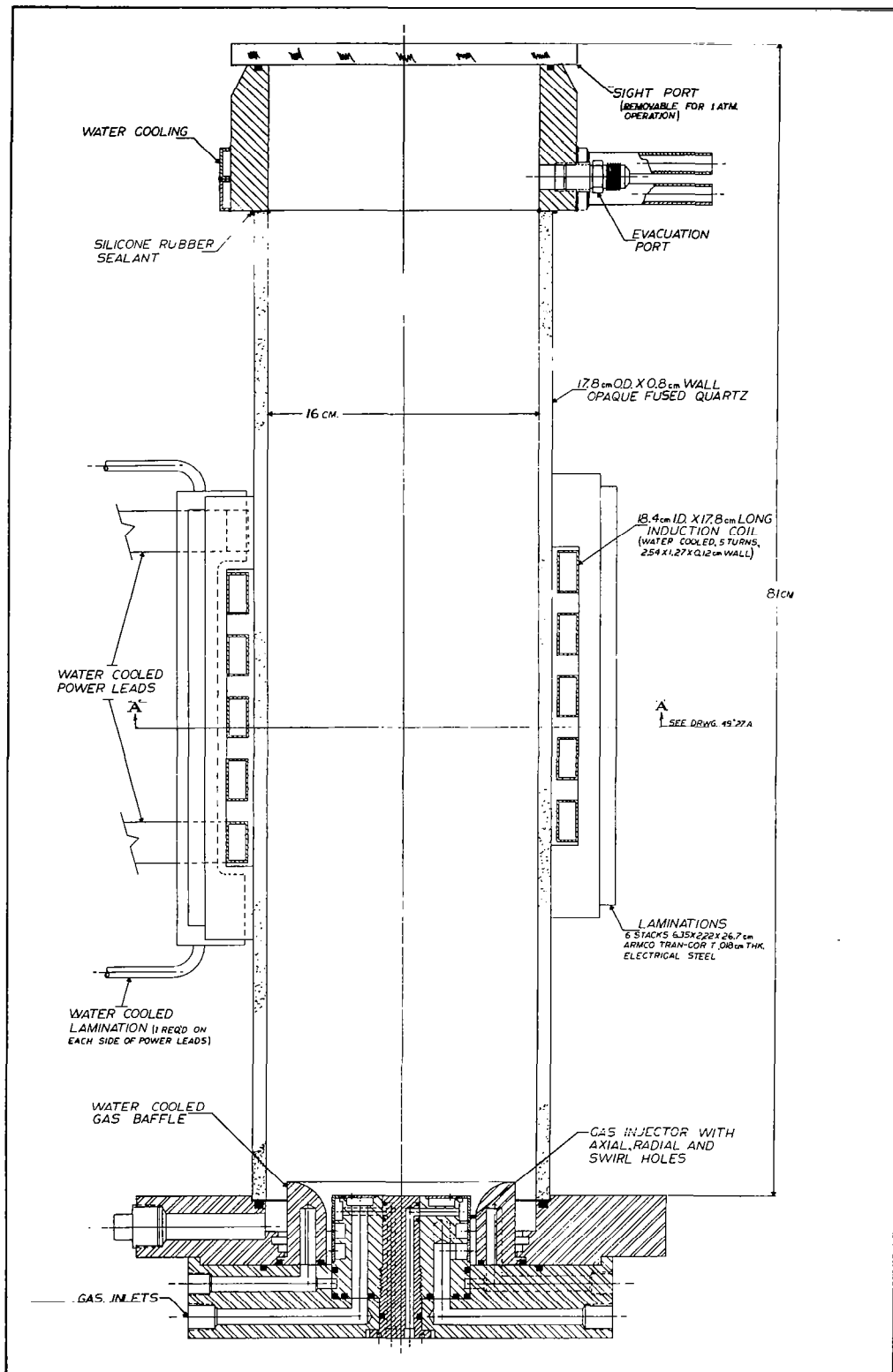
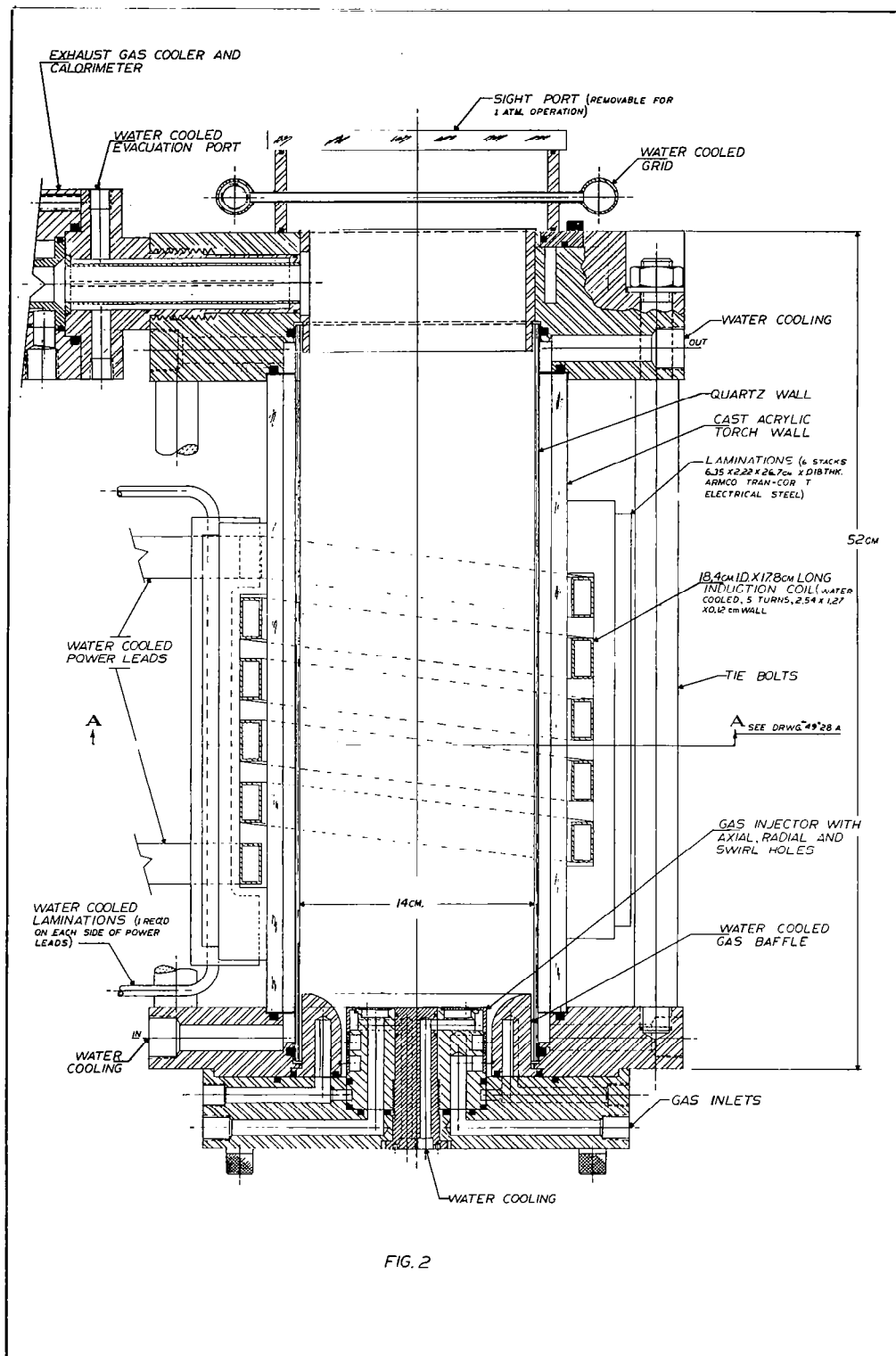


FIG. 1

14cm I.D. WATER COOLED TORCH



30 cm I.D. UNCOOLED TORCH

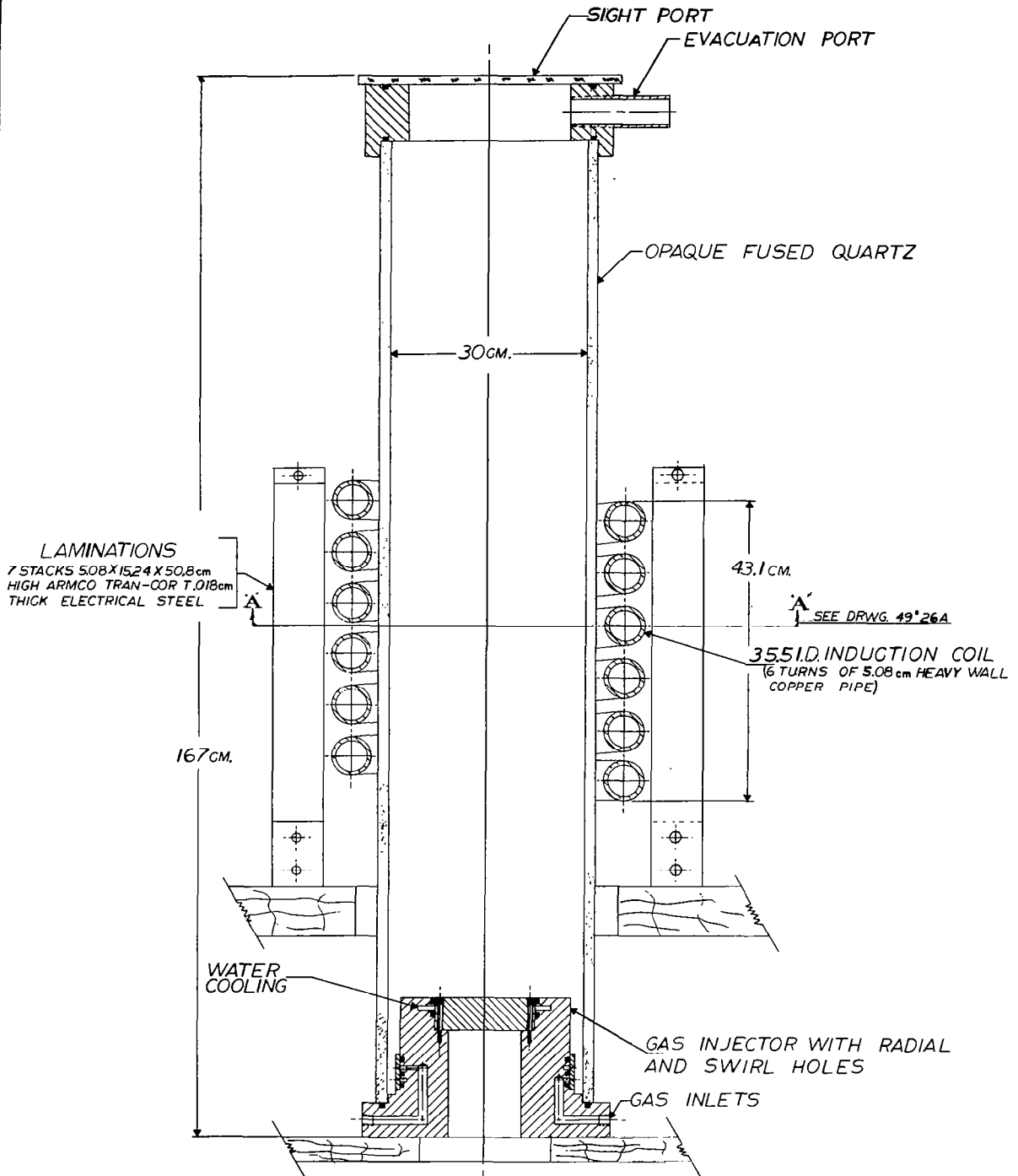


FIG. 3

TEST FACILITY FOR 9,600 Hz TESTS

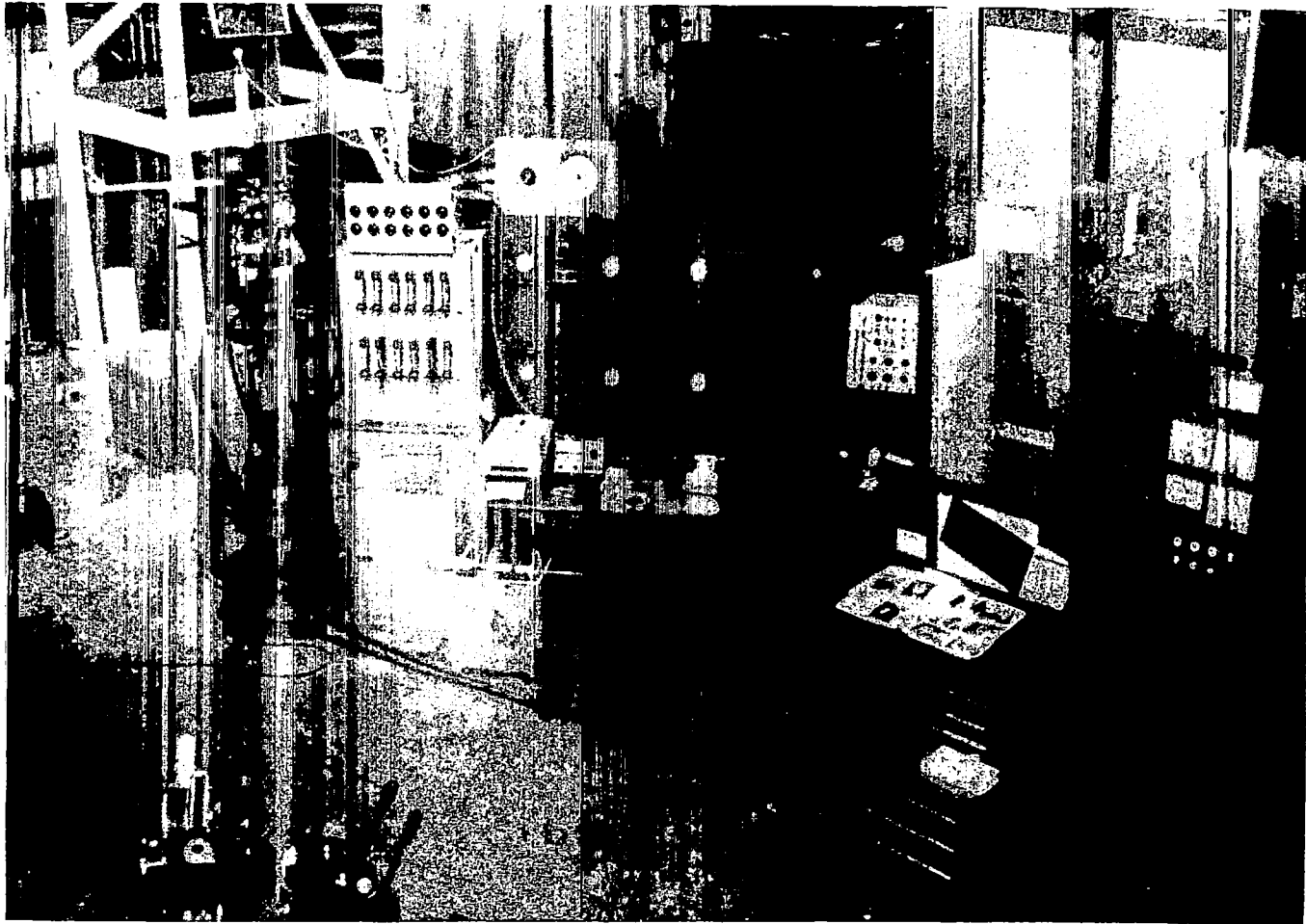


FIG. 4

BUSS CONNECTIONS TO 14cm I.D. WATER COOLED TORCH FROM CAPACITOR BANK

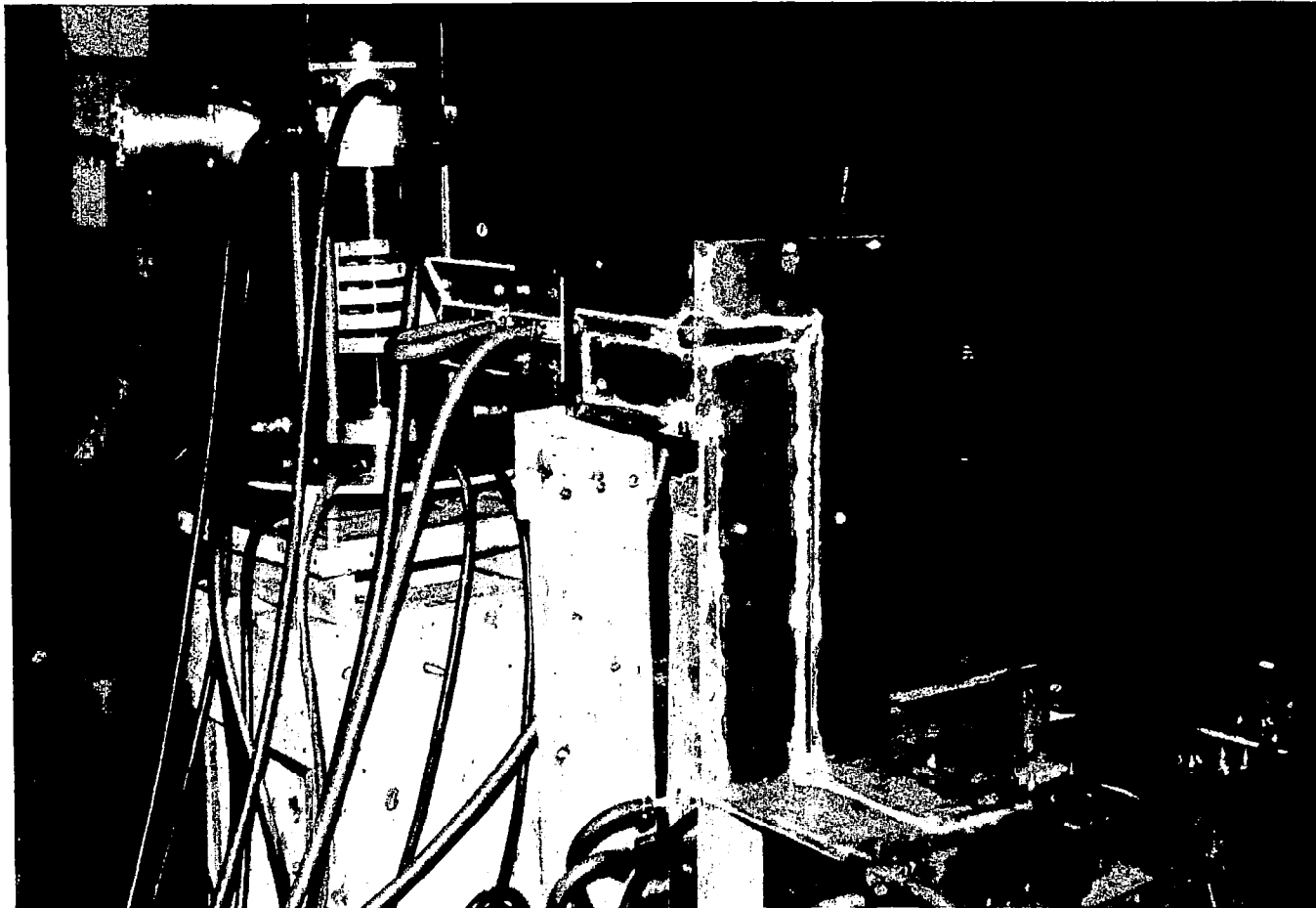


FIG. 5

VISICORDER TRACE FOR START-UP OF 14 cm I.D. WATER COOLED TORCH AT 9600 HERTZ

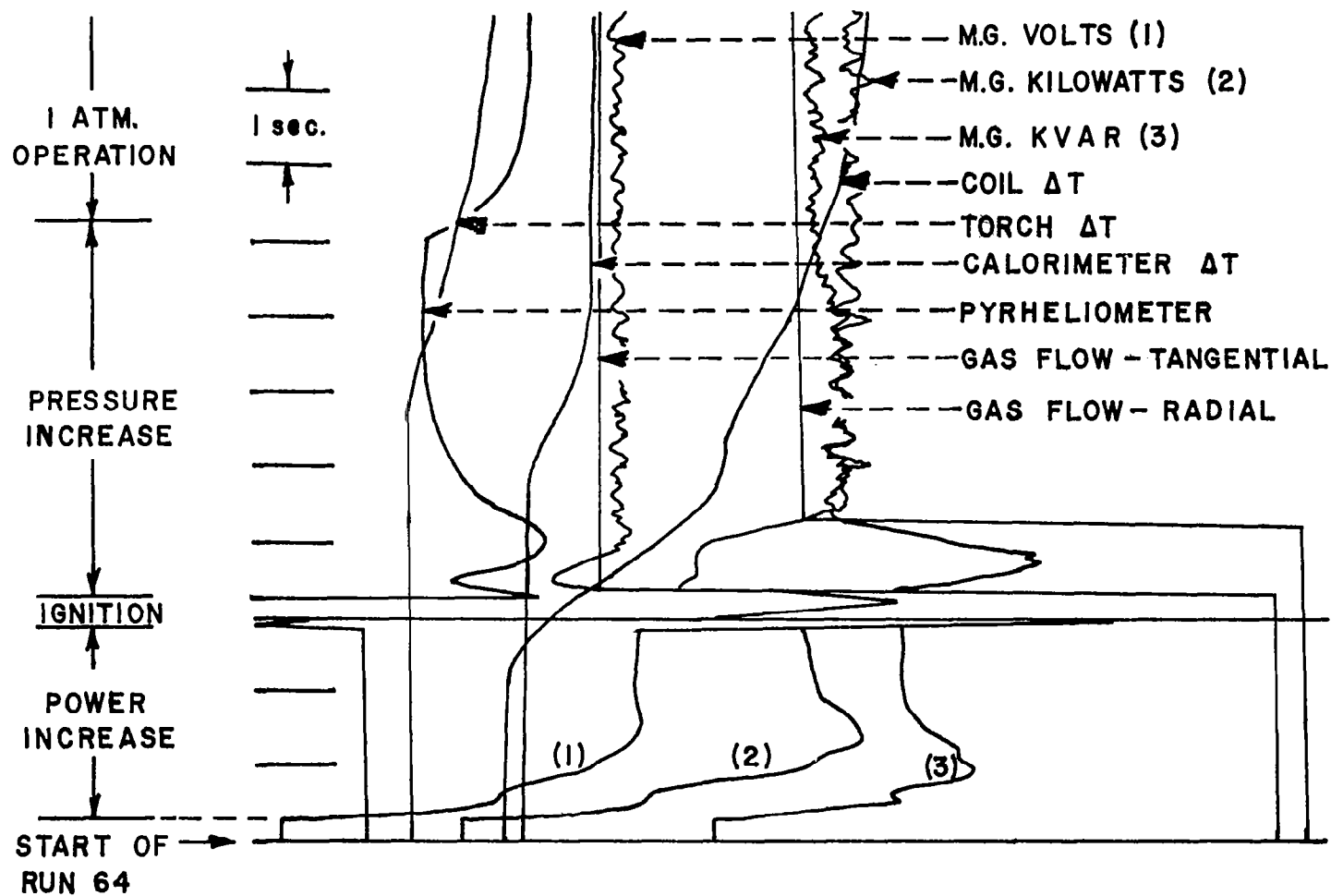


FIG. 6

VISICORDER TRACE FOR START-UP OF 30 cm I.D. UNCOOLED TORCH AT 9600 HERTZ

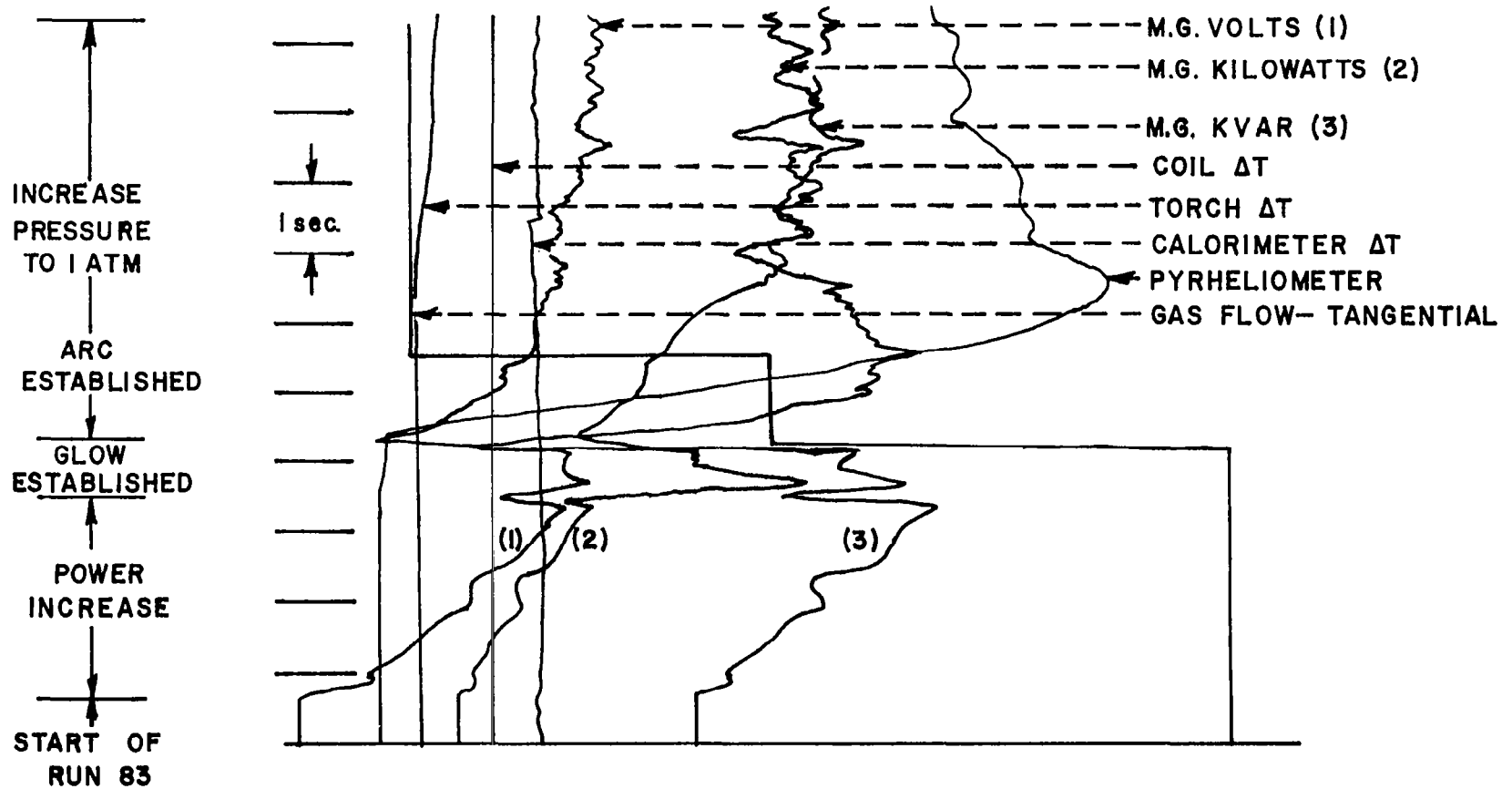


FIG. 7

VISICORDER TRACE FOR MINIMUM SUSTAINING POWER DETERMINATIONS FOR RUN 61

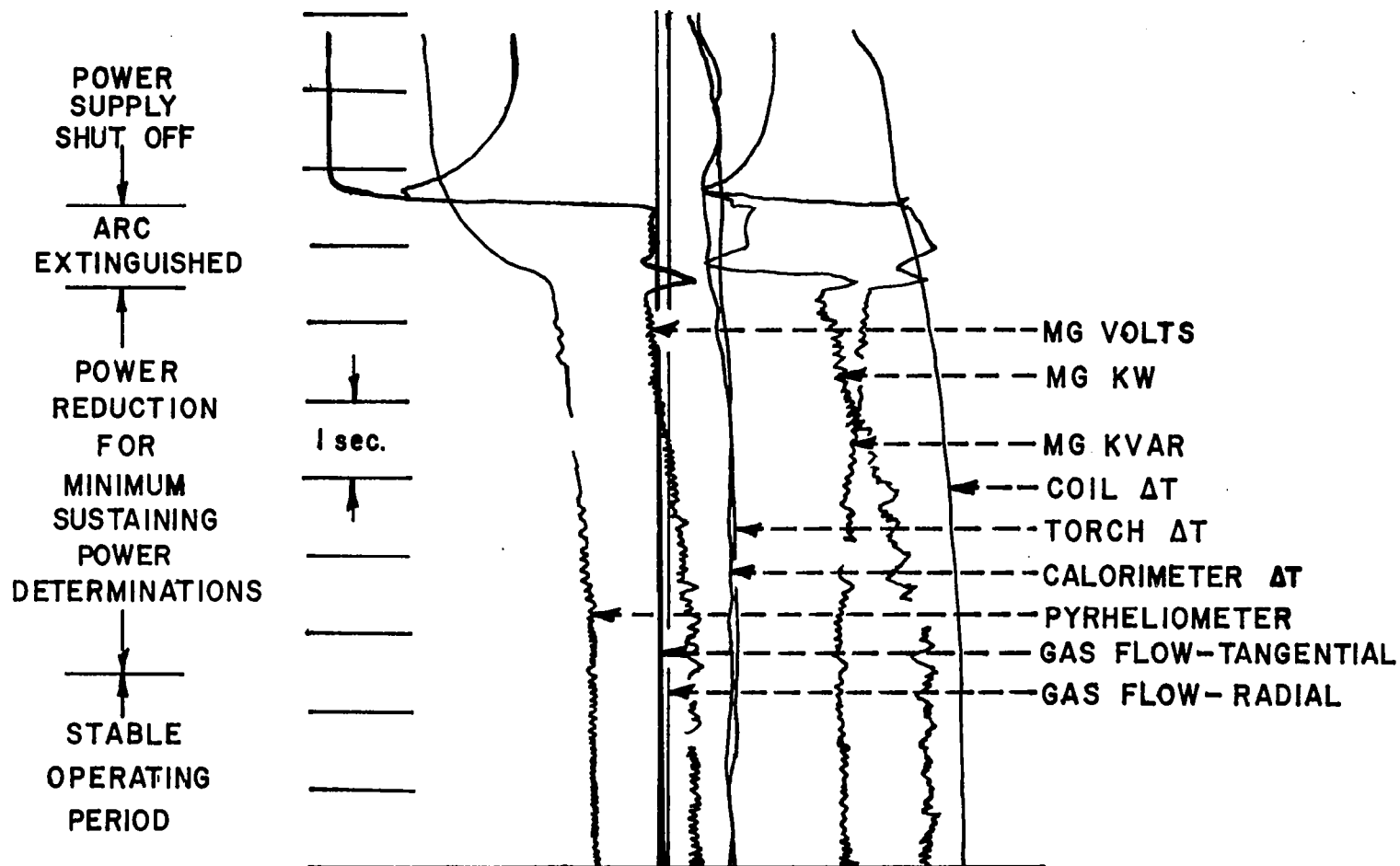


FIG. 8

TEST INSTRUMENTATION SET-UP

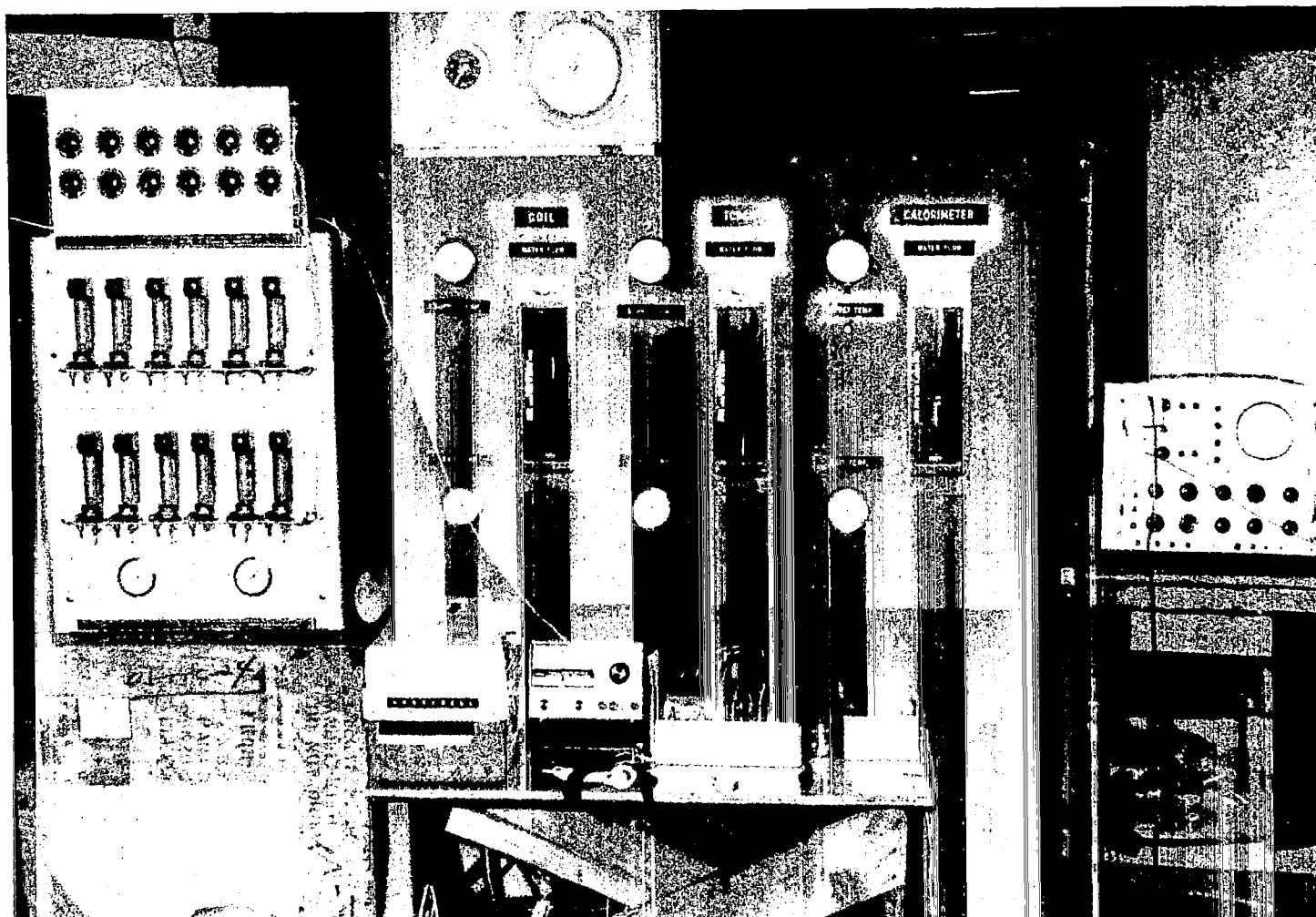


FIG. 9

16 cm I.D. UNCOOLED TORCH

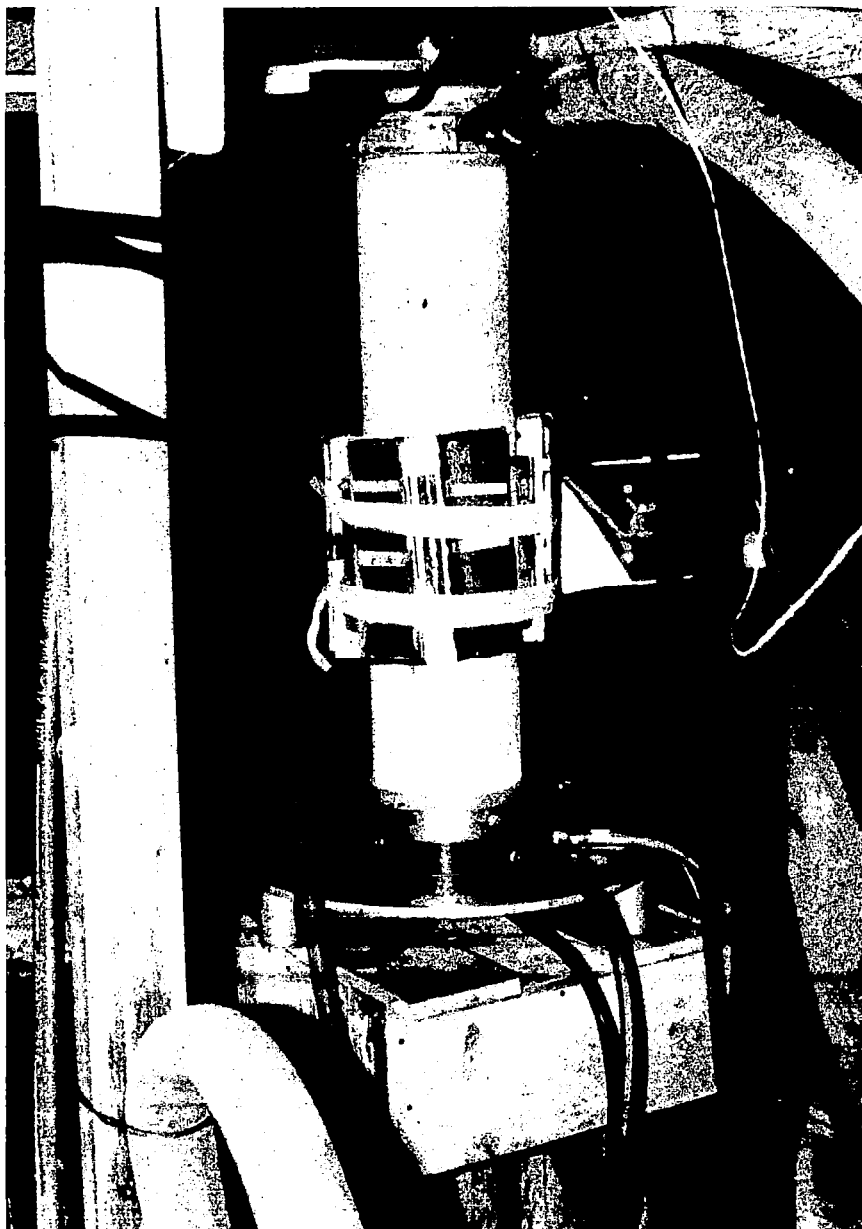


FIG. 10

14cm I.D. WATER COOLED TORCH

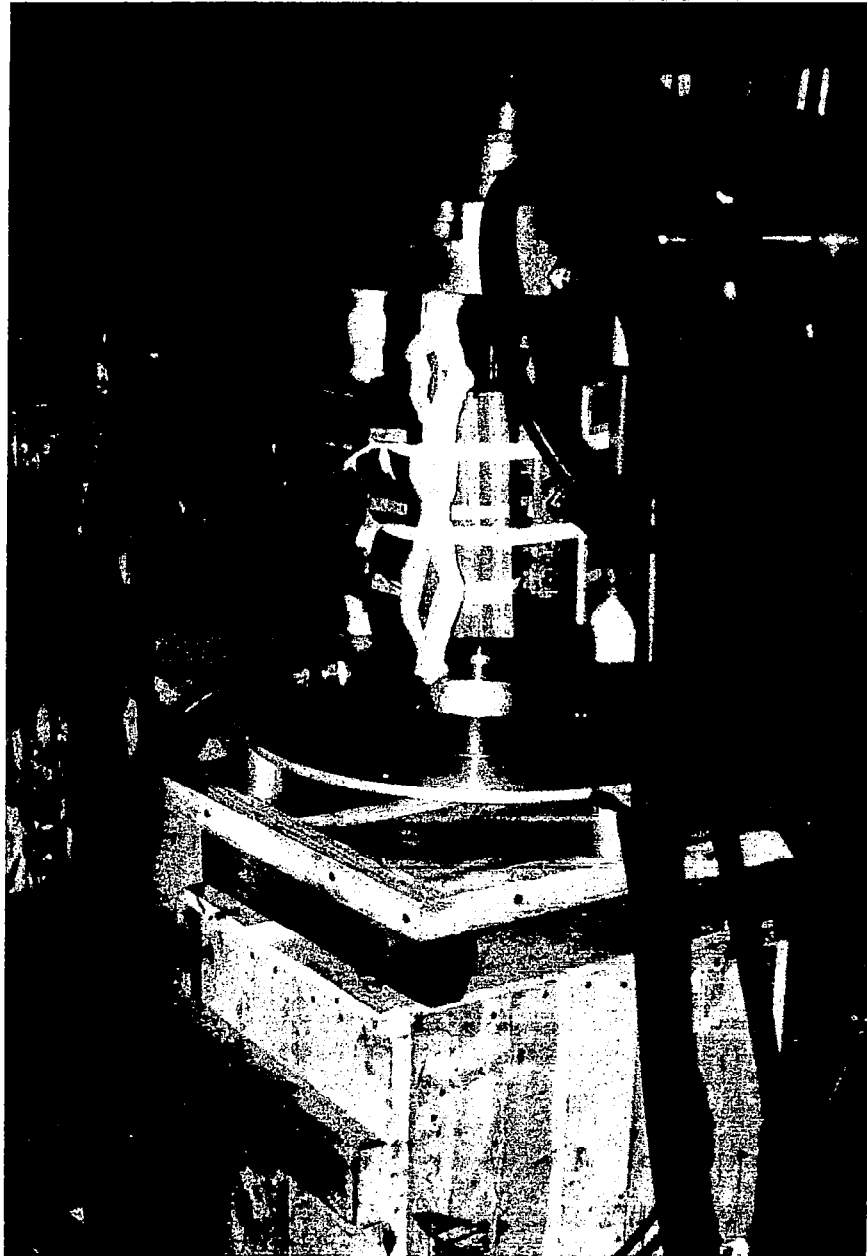


FIG. II

14 cm I.D. WATER COOLED TORCH IN OPERATION



FIG. 12

30cm I.D. UNCOOLED TORCH

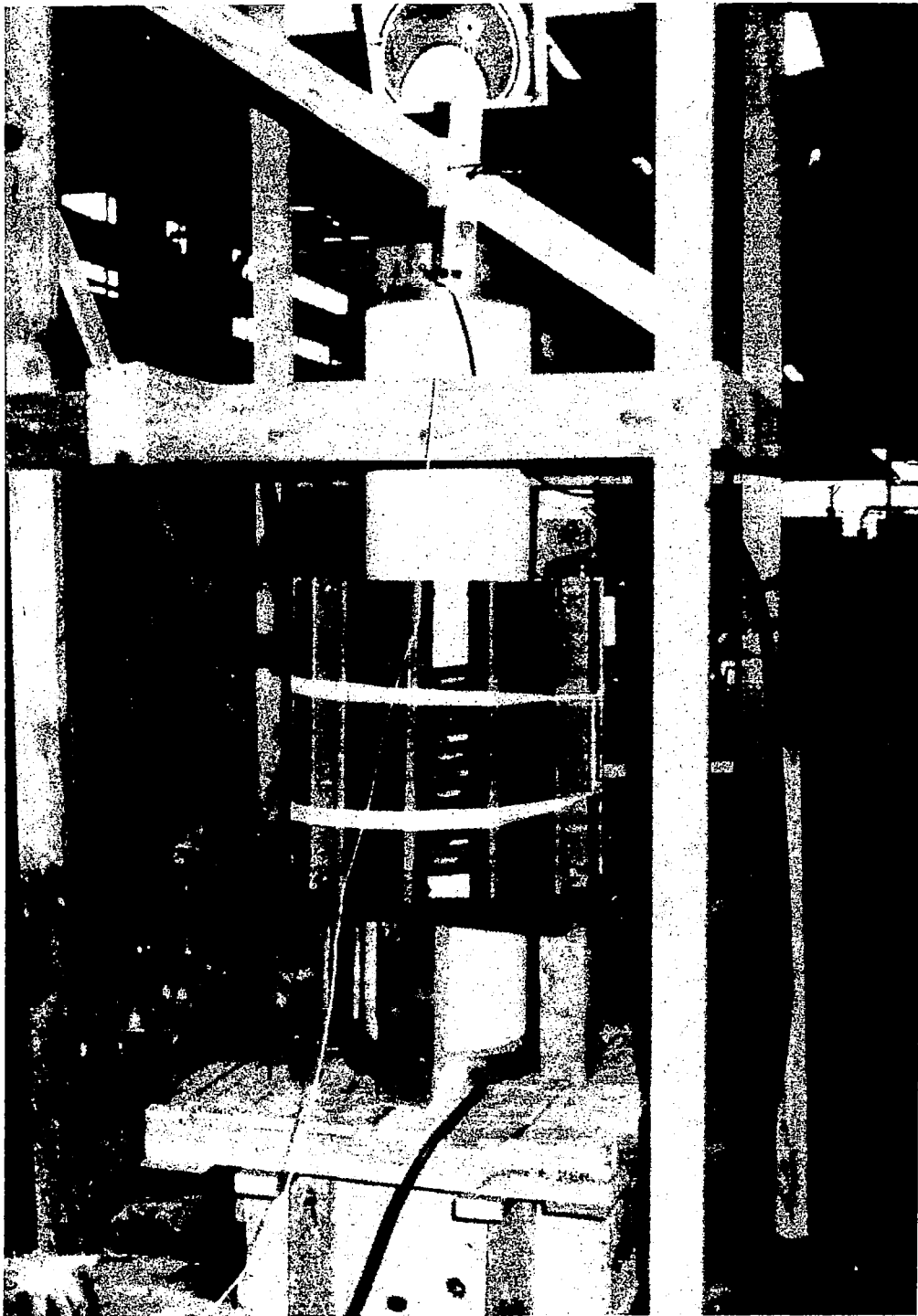


FIG. 13

30 cm I.D. TORCH IN OPERATION

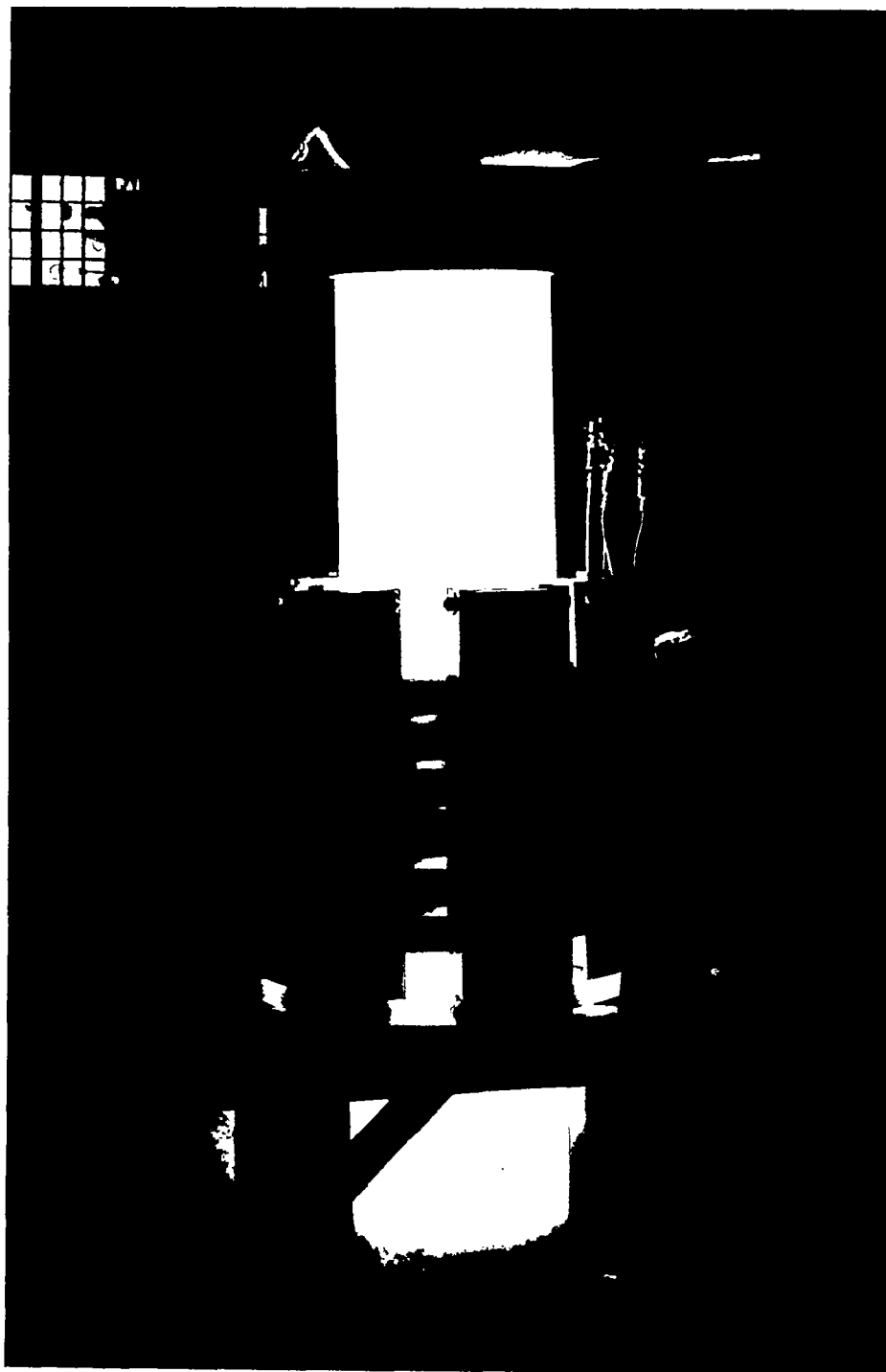


FIG.14

MINIMUM SUSTAINING POWER AT REDUCED PRESSURE

(ARGON PLASMA AT 9,600 Hz)

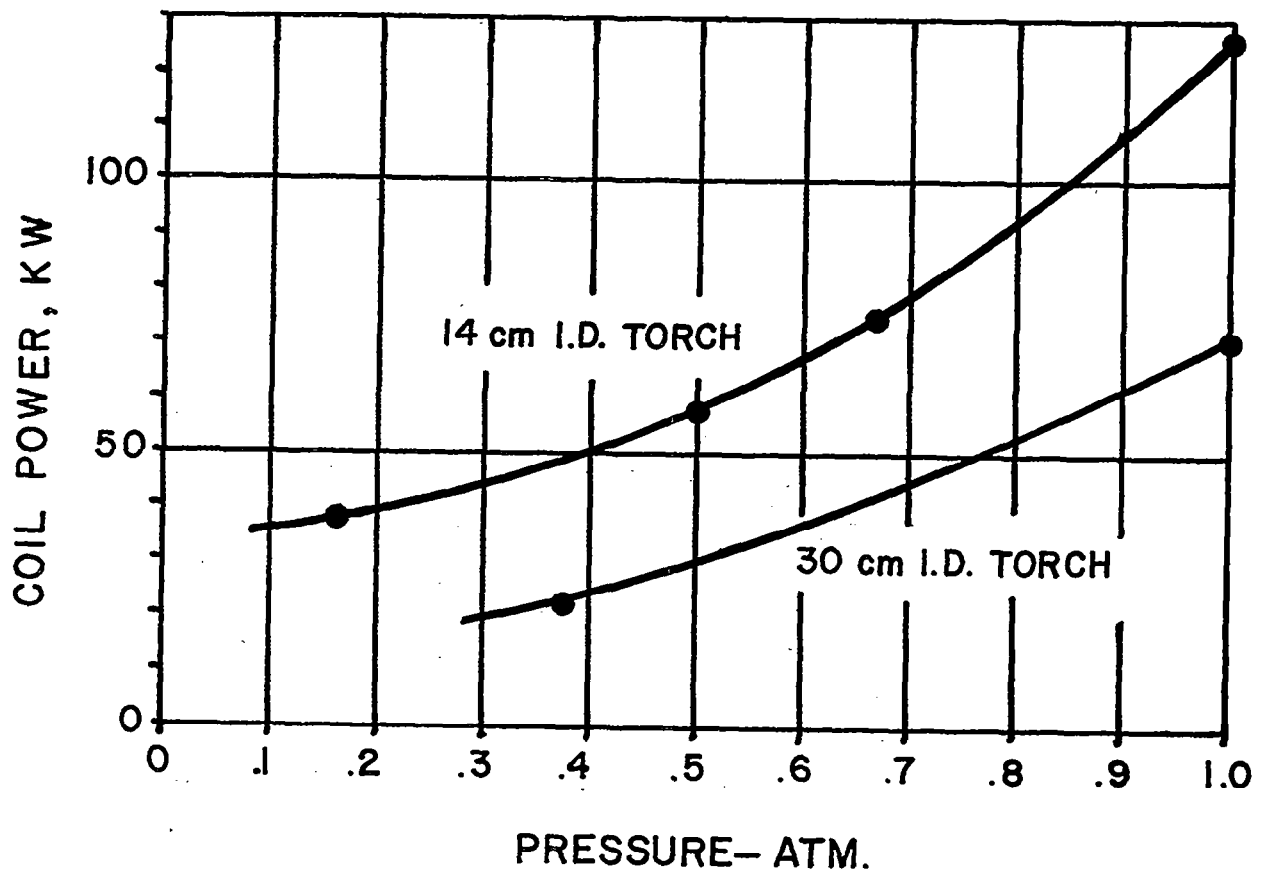


FIG. 15

POWER TO GAS AT MINIMUM SUSTAINING POWER AND REDUCED PRESSURE

(ARGON PLASMA AT 9,600 Hz)

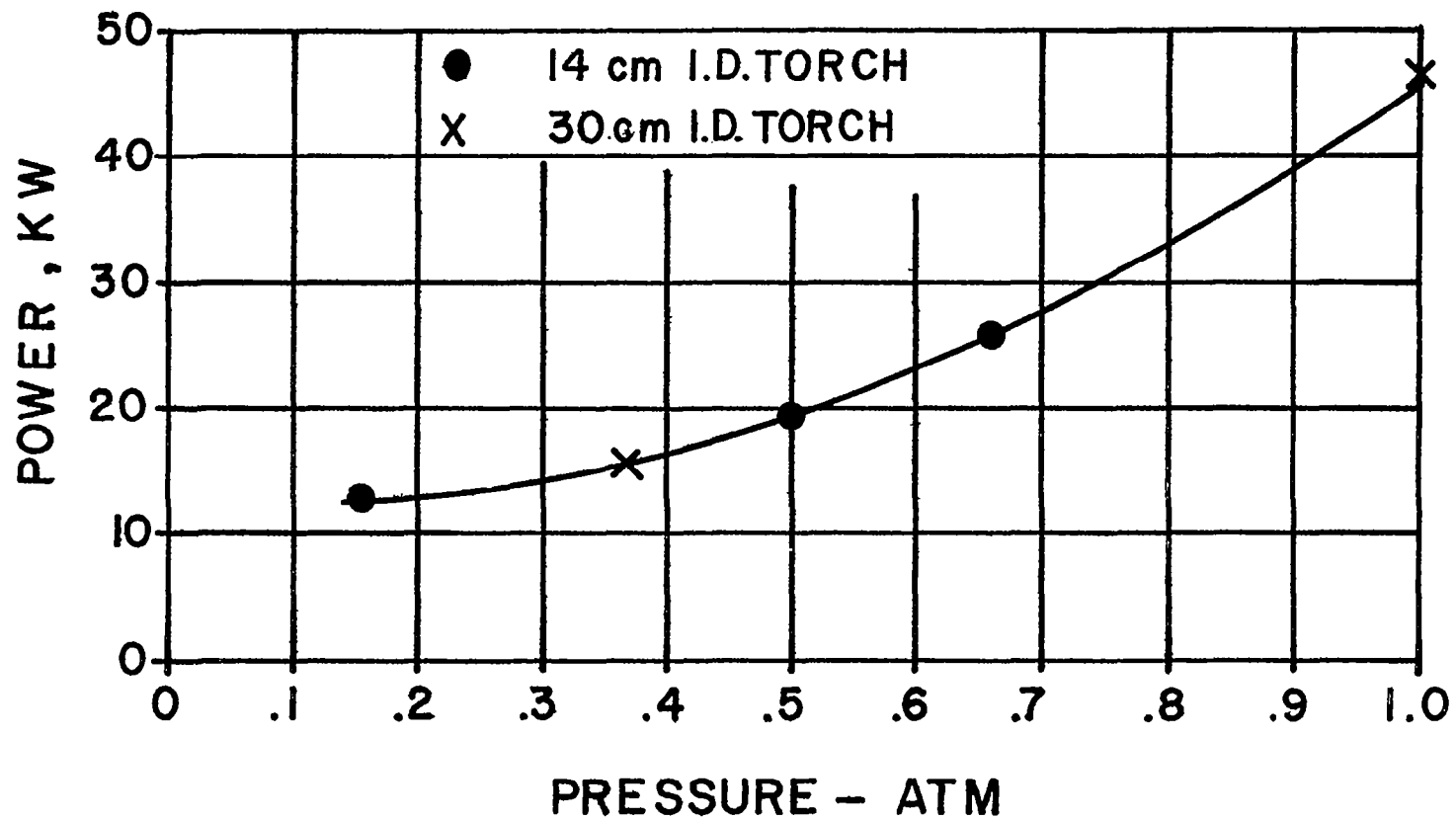


FIG. 16

MINIMUM SUSTAINING POWER vs GAS FLOW

(ARGON PLASMA AT 9,600Hz AND ONE ATMOSPHERE)

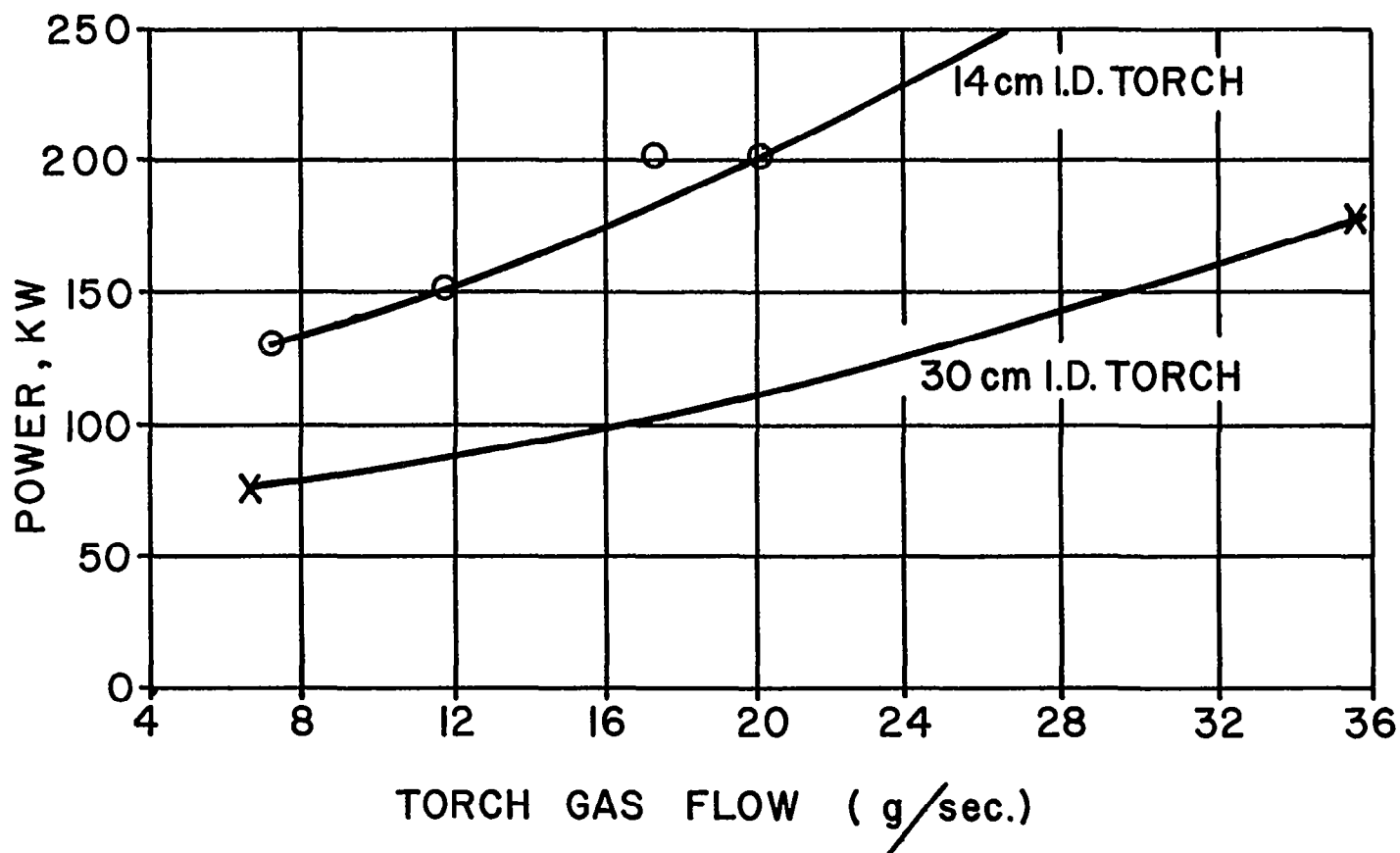


FIG.17

POWER TO THE GAS AT M.S.P. vs GAS FLOW

(ARGON PLASMA AT 9,600Hz AND ONE ATMOSPHERE)

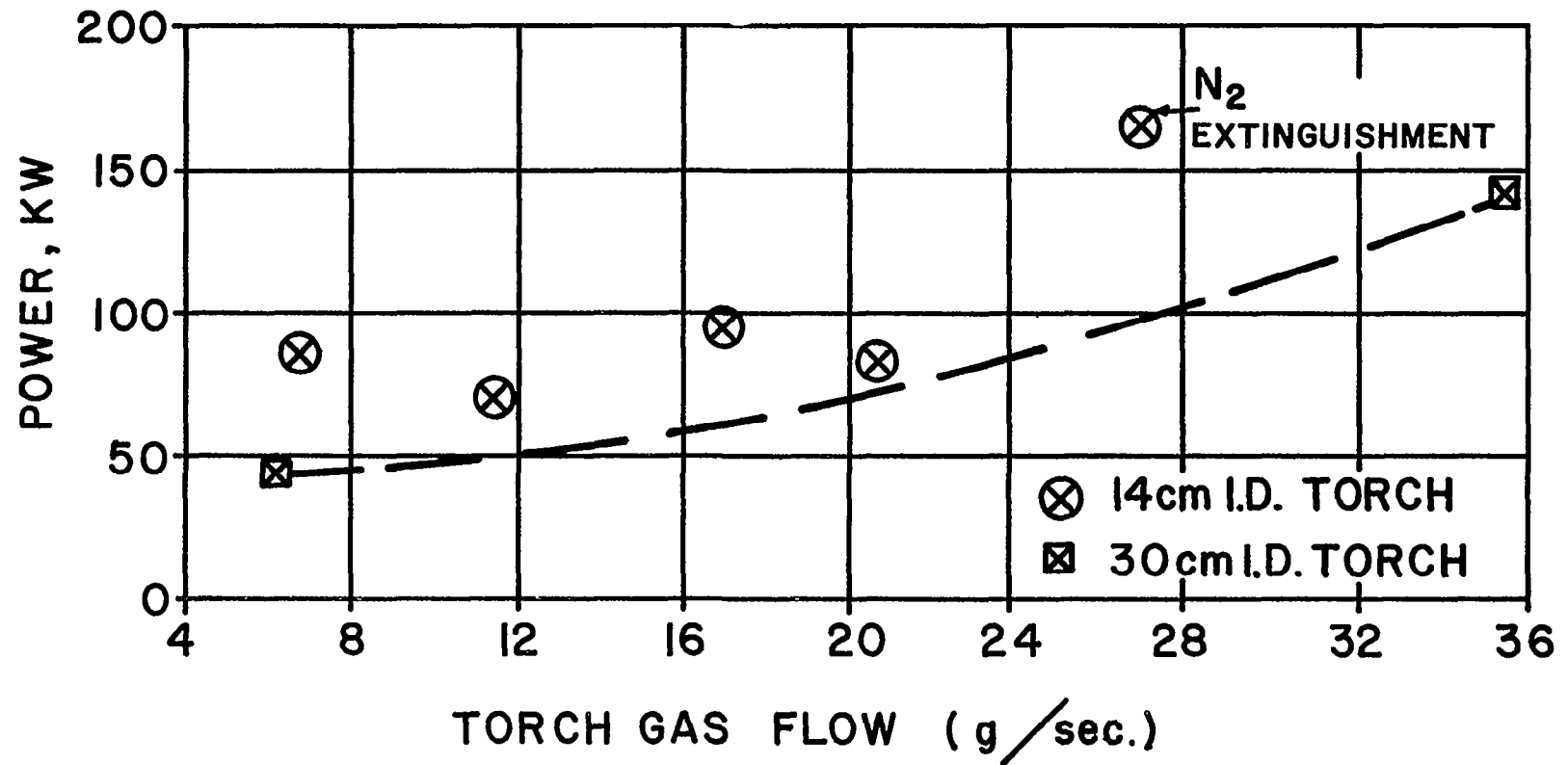


FIG. 18

TOTAL ELASTIC-COLLISION CROSS SECTION DUE TO ELECTRON IMPACT AT $t=0^{\circ}\text{C}$ AND $P=1$ TORR

(FROM REFERENCE 4)

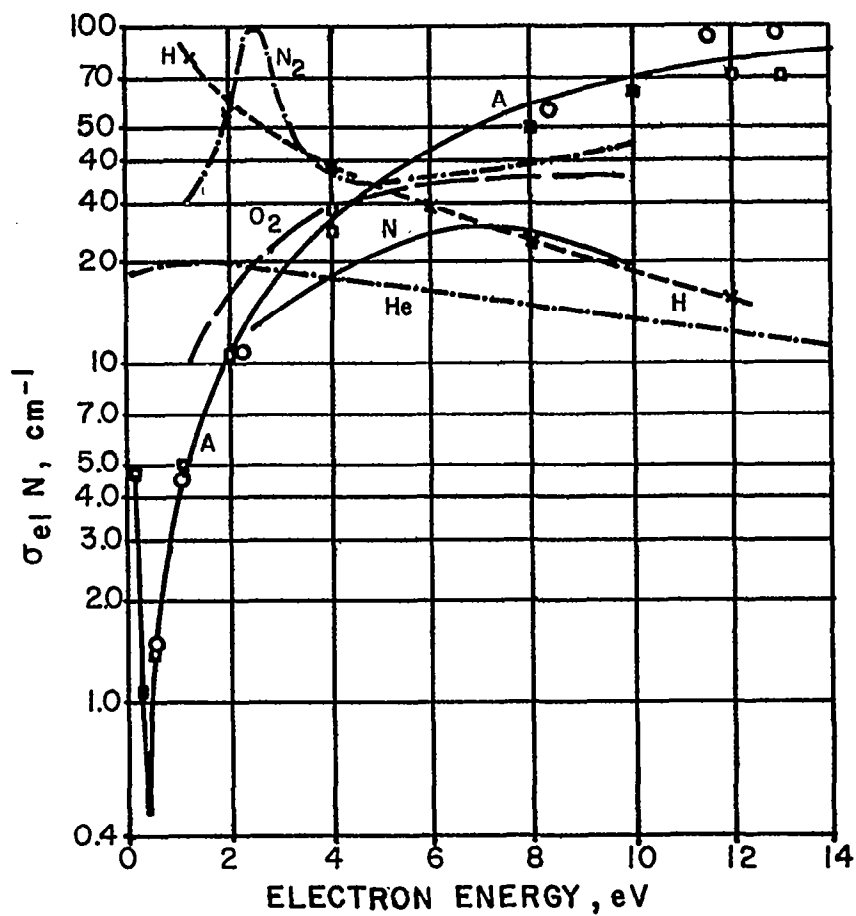


FIG. 19

LOAD RESISTANCE FACTOR AS A FUNCTION OF PLASMA DIAMETER TO REFERENCE DEPTH RATIO

(FROM REFERENCE 1, FIGURE 34)

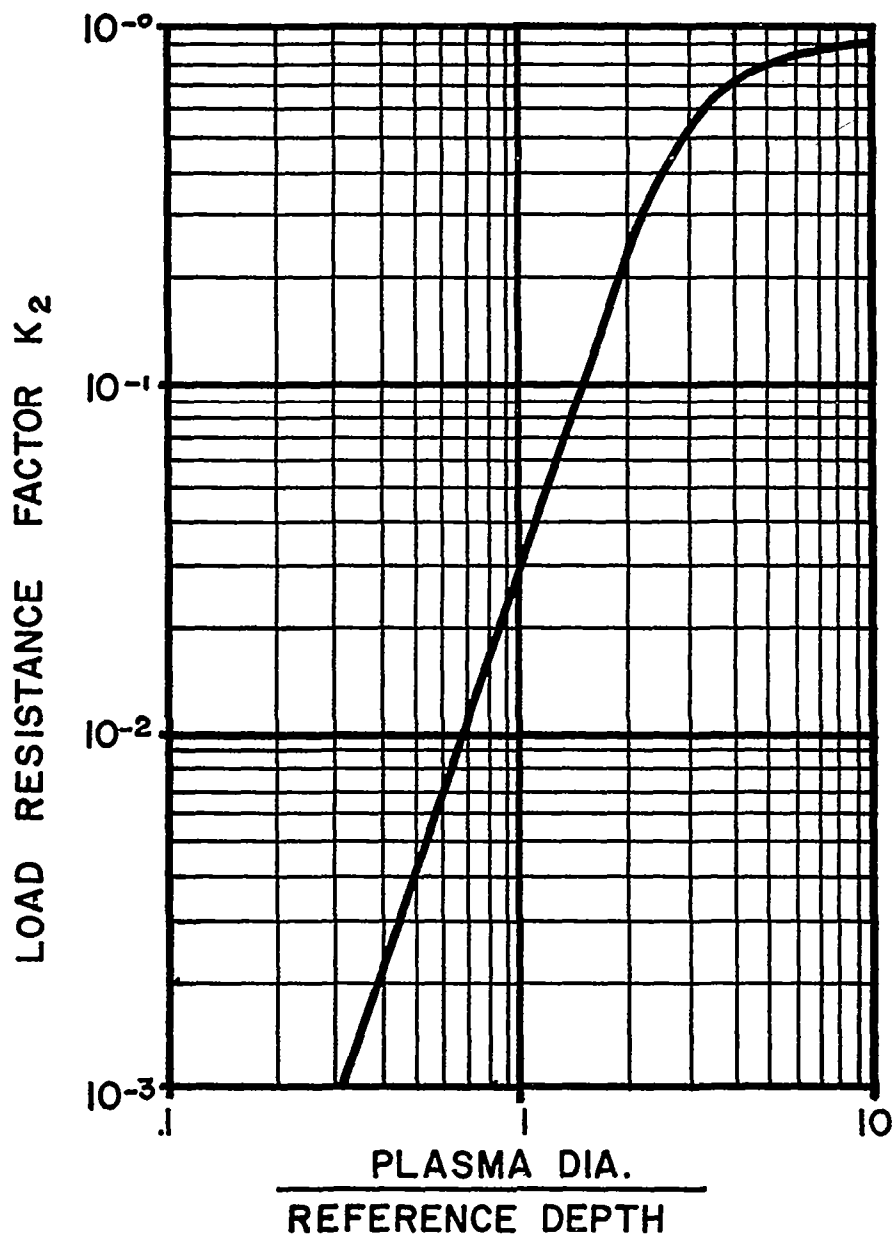


FIG. 20